

This article was downloaded by:

On: 30 January 2011

Access details: Access Details: Free Access

Publisher Taylor & Francis

Informa Ltd Registered in England and Wales Registered Number: 1072954 Registered office: Mortimer House, 37-41 Mortimer Street, London W1T 3JH, UK



## Spectroscopy Letters

Publication details, including instructions for authors and subscription information:

<http://www.informaworld.com/smpp/title~content=t713597299>

### MINDO/3 CI Study of NCO Spectrum and the Chemiluminescent Reaction $N\ CO \rightarrow NCO\ h$

B. F. Minaev<sup>a</sup>; N. M. Ivanova<sup>a</sup>; Z. M. Muldaahmetov<sup>a</sup>

<sup>a</sup> Karaganda State University, Karaganda, USSR

**To cite this Article** Minaev, B. F. , Ivanova, N. M. and Muldaahmetov, Z. M.(1989) 'MINDO/3 CI Study of NCO Spectrum and the Chemiluminescent Reaction N CO → NCO h', Spectroscopy Letters, 22: 7, 901 — 923

**To link to this Article: DOI:** 10.1080/00387018908053945

**URL:** <http://dx.doi.org/10.1080/00387018908053945>

## PLEASE SCROLL DOWN FOR ARTICLE

Full terms and conditions of use: <http://www.informaworld.com/terms-and-conditions-of-access.pdf>

This article may be used for research, teaching and private study purposes. Any substantial or systematic reproduction, re-distribution, re-selling, loan or sub-licensing, systematic supply or distribution in any form to anyone is expressly forbidden.

The publisher does not give any warranty express or implied or make any representation that the contents will be complete or accurate or up to date. The accuracy of any instructions, formulae and drug doses should be independently verified with primary sources. The publisher shall not be liable for any loss, actions, claims, proceedings, demand or costs or damages whatsoever or howsoever caused arising directly or indirectly in connection with or arising out of the use of this material.

MINDO/3 CI STUDY OF NCO SPECTRUM AND THE  
CHEMILUMINESCENT REACTION  $N + CO \rightarrow NCO + h\nu$

**Key words:** NCO radical, potential energy surfaces, chemiluminescence, spin-orbit coupling

B.F.Minaev, N.M.Ivanova, Z.M.Muldaahmetov

Karaganda State University, Karaganda, 470074,  
USSR

**ABSTRACT**

The mechanism of chemiluminescence in the reaction  $N + CO \rightarrow NCO$  (1) and the electronic spectrum of NCO radical have been investigated by means of MINDO/3 CI method. The potential energy curves for the ground and some excited doublet and quartet states have been built along the linear and nonlinear (angle NCO is equal to  $150^\circ$ ) reaction coordinates. The reaction channels  $N(^4S) + CO(^1\Sigma^+)$ ,  $N(^2D) + CO(^1\Sigma^+)$  and  $N(^2P) + CO(^1\Sigma^+)$  have been discussed in detail. The spin-orbit coupling (SOC) constants for  $^2\Pi$  states and nonadiabatic SOC matrix elements  $\langle ^4\Sigma^- | H_{soc} | X^2\Pi \rangle$  have been calculated.

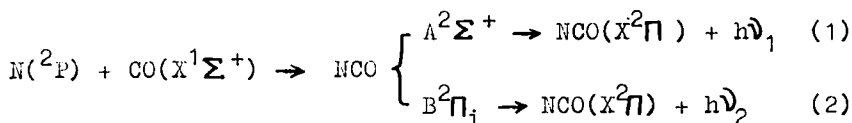
**INTRODUCTION**

The NCO radical and its chemiluminescence have been the subject of a number of experimental investigations [4,

8, 11, 15, 22]. Dixon [1, 2] has observed a transient species in emission spectra during flash photolysis of isocyanic acid HNCO vapor and assigned the bands to linear NCO radical. The same electronic transition in the visible and UV regions (4500-3600 Å) has been observed in absorption and ascribed to  $\tilde{A}^2\Sigma^+$  -  $\tilde{X}^2\Pi$  transition [1]. From an analysis of the vibrational and rotational structure Dixon has determined the values of all vibrational frequencies for  $\tilde{A}^2\Sigma^+$  state and the bending frequency for the ground state, the rotational and spin-orbit coupling (SOC) constants ( $A = -95,59\text{cm}^{-1}$ ), anharmonic and Renner-Teller parameters for the  $\tilde{X}^2\Pi$  state. Dixon was unable to assign the bond lengths, but he obtained the upper limits of their sum as  $2,408\text{\AA}$  ( $\tilde{X}^2\Pi$ ) and  $2,369\text{\AA}$  ( $\tilde{A}^2\Sigma^+$ ). In another paper [2] Dixon has analysed the UV spectrum 2650-3200 Å, which was attributed to a  $\tilde{B}^2\Pi$  -  $\tilde{X}^2\Pi$  electronic transition with a progression of the upper state stretching vibrations;  $A(\tilde{B}^2\Pi_1) = -30,8\text{cm}^{-1}$ ,  $R_{\text{NC}} + R_{\text{CO}} < 2,45\text{\AA}$ . The radical possesses a linear equilibrium structure in all studied electronic states. The papers [1, 2] perform the classical analysis of linear-linear transitions [3]. Milligan and Jacox [4] have studied the UV and IR spectra of NCO radical, trapped in argon matrix, and determined the values of all three vibrational frequencies for the  $X^2\Pi$  state. The gas phase ESR technique has been developed by Carrington et al. [5, 6] and the effective hamiltonian for NCO (including SOC, nuclear hyperfine interactions and rovibronic parameters) has been obtained [6]. Saito and Amano [7] observed the rotational spectrum of NCO

radical by means of a Stark modulated microwave spectrometer. Analysing the  $\Lambda$ -doubling constants, the authors came to the conclusion that the  $X^2\Pi$  state was perturbed by the  $\tilde{A}^2\Sigma^+$  state. More recently, the laser excited fluorescence spectrum of NCO has been studied [8-11]; the lifetimes and energies of several rovibronic levels have been determined.

Some recent experimental works were devoted to NCO kinetics [12-14]. Excitation of the emission spectrum of NCO in solid matrices condensed at 4 K have been interpreted as a result of chemiluminescent reaction [15]



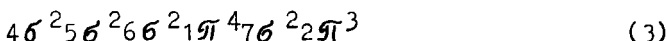
In contrast to the extensive experimental work described above there exist only a few theoretical studies to the NCO radical. Thomson and Wishart [16] have investigated the geometry of the ground state within the restricted Hartree-Fock SCF approximation with a double-zeta basis set and added polarisation functions; they obtained the following bond lengths:  $R_{N-C} = 1,2255 \text{ \AA}$  and  $R_{C-O} = 1,1334 \text{ \AA}$ . Vertical electronic transitions in NCO have been calculated within the semiempirical INDO/S CI approximation by Čarsky, Kuhn and Zahradník [17]. They predicted  $\tilde{a}^4\Pi$  quartet state to be the second excited state in NCO spectrum and also a number of new  $^2\Pi - ^2\Pi$  transitions. Ab initio MRD-CI study of the Renner-Teller effect and SOC in the  $X^2\Pi$  ground state of NCO [18] and SCF 6-31\*G investigation

of the structure and electron affinity of NCO isomers [19] have been performed recently.

No theoretical studies of the NCO electronic spectrum with optimized excited state geometries have been published to our knowledge so far. In this paper we present the results of semiempirical MINDO/3 CI calculations on potential energy surfaces (PES) cross sections for a number of doublet and quartet states along the reaction  $N + CO \rightarrow NCO$ . Because of the crude MINDO/3 approximations, the results are only qualitative in manner.

#### METHOD OF CALCULATION

The ground state  $X^2\pi$  electronic configuration of NCO ( $G_0$  -configuration)



was treated by MINDO/3 [20] restricted Hartree-Fock SCF procedure within the Ellison-Mattheu approximation [21]. The N-C distance was fixed at different values between 1,1 Å and 2,6 Å with a step of 0,1 Å. The other parameters ( $R_{CO}$  and angle N-C-O) were optimized at each point. The PES of the single configuration (3) is shown in Fig.1 by a dotted line. On this SCF MO basis the configurational interaction (CI) [17,22] has been calculated (full lines in Fig1). 42 doublet and 16 quartet (Q) configurations are taken into account. (All single excitations accounted, excepting two lowest occupied MO  $4\sigma$ ,  $5\sigma$  with very low energy;  $C_2$ ,  $C_3$  and Q configurations include  $4 \times 4$  excitations).

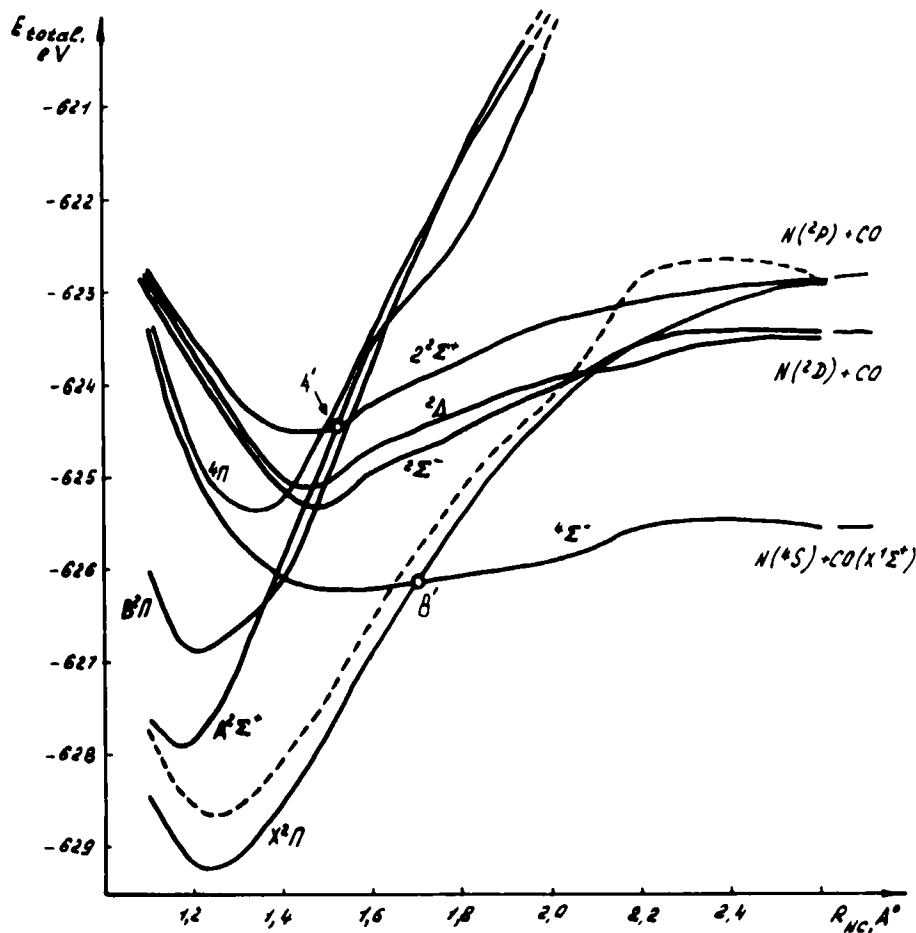


Fig. 1. The potential energy curves of linear NCO for the lowest states of each symmetry and multiplicity.

## RESULTS AND DISCUSSION

The ground state geometry optimization gives a linear molecular geometry with the optimal values for  $R_{N-C} = 1,237 \text{ \AA}$  and  $R_{C-O} = 1,178 \text{ \AA}$ . Their sum ( $2,415 \text{ \AA}$ ) is in a good agreement with experimental ( $2,408 \text{ \AA}$ ) [3] and ab initio ( $2,43 \text{ \AA}$ ) [18] values.

The calculated PES for a number of the excited states along the reaction  $N + CO$  are shown in Fig.1. The lowest dissociation limits ( $R_{NC} = 2,6 \text{ \AA}$ ) correspond to  $N(^4S) + CO$ ,  $N(^2D) + CO$  and  $N(^2P) + CO$  states of reagents (CO is in the ground  $X^1\Sigma^+$  state); the other excited dissociation limits ( $N^+ + CO^-$ ,  $N + CO(^1,3\Pi, ^1,3\Sigma^-, \text{etc})$ ) are not shown in Fig.1. It is easy to see, that our crude CI approximation reproduces qualitatively well the known dissociation limits for nitrogen atomic configurations ( $^4S$ ,  $^2D$ ,  $^2P$ ). Experimental values  $E(^2D) - E(^4S)$  and  $E(^2P) - E(^2D)$  energy differences are equal to 2,38 eV and 1,19 eV [23]; MINDO/3 CI values are 2,1 eV and 0,91 eV, respectively. The experimental dissociation energy  $D_e(N-CO)$  is equal to 2,10  $\pm 0,15$  eV (the exact state product is not known) [23], but MINDO/3 CI calculations highly overestimate this value (5,7 eV for  $N(^2D) + CO(^1\Sigma^+)$  limit and 3,6 eV for  $N(^4S) + CO(^1\Sigma^+)$  limit. We shall show later that the last limit must correspond to the experimental one.) On the other hand, the electronic transition energies in NCO radical are underestimated in our calculation. The MINDO/3 parametrization doesn't take into account the differences bet-

ween  $\sigma$ - and  $\pi$ -types of overlapping  $S_{pp}$ , and  $\beta\pi\pi - \beta\sigma\sigma$  resonance integrals. So the MINDO/3 method underestimates the energies of  $\sigma-\pi$  and  $\pi-\pi$  electronic transitions. INDO/S method [17] accounts  $\sigma-\pi$  differences much better and rather well reproduces the observed spectra. For comparison we give the INDO/S CI [17] results on the ground state MO (Table 1) and vertical electronic transition of NCO radical ( $R_{NC} = 1,23 \text{ \AA}$ ,  $R_{CO} = 1,13 \text{ \AA}$ , Table 2). As is seen from Table 2, the MINDO/3 CI transition energies differ from that obtained by experiments and INDO/S CI calculations. All the MINDO/3 CI excited states of NCO lie lower than experimental ones, except for the  $^4\Pi$  state. This is the result of the above marked shortage of the MINDO/3 method. In our calculations the  $^4\Sigma^-$  state is the first excited quartet state in contrast to INDO/S results [17]. The underestimation of the electronic transition energies does not influence on the qualitative results, because the state succession is true.

Fig. 1 shows the change of the minimum position on the potential energy curves of the excited states of NCO. The potential minimum of  $\tilde{\Lambda}^2\Sigma^+$  state is located at a shorter  $R_{NC}$  distance than the minimum position of the  $\tilde{\chi}^2\Pi$  state. This fits well to the experimental sum ( $R_{NC} + R_{CO} \leq 2,369 \text{ \AA}$ ) [3]. The highest excited states have a longer N-C bond length than the ground state one.

The lowest excited  $\Lambda^2\Sigma^+$  state of NCO corresponds mainly to the electron transfer from  $7\sigma$  to  $2\pi$  MO and has

Table 1.  
 The energies  $\epsilon_i$  (ev) and LCAO coefficients of MO's in the ground  $X^2\pi$  state  
 of NCO obtained by INDO/S [17] method

| $\mu$ | $\epsilon_i$ | 4s     | 5s     | 6s     | 1 $\pi$ | 7s | 2 $\pi$ | 3 $\pi$ | 8s | 9s           |
|-------|--------------|--------|--------|--------|---------|----|---------|---------|----|--------------|
| C     | 2s           | -0,509 | -0,396 | -0,323 | -0,168  |    |         |         |    | -0,664 0,103 |
|       | 2p $\pi$     | -0,316 | 0,461  | -0,144 | 0,307   |    |         |         |    | 0,076 0,753  |
| N     | 2s           | -0,113 | -0,717 | 0,328  | 0,493   |    |         |         |    | 0,265 0,227  |
|       | 2p $\pi$     | -0,094 | -0,260 | -0,233 | -0,683  |    |         |         |    | 0,560 0,297  |
| O     | 2s           | -0,739 | 0,219  | 0,510  | -0,144  |    |         |         |    | 0,177 -0,306 |
|       | 2p $\pi$     | 0,271  | 0,003  | 0,673  | -0,383  |    |         |         |    | -0,372 0,435 |

Table 2  
Excitation energies ( in eV) of NCO radical

| State                   | Excitation energy |                        |                       |
|-------------------------|-------------------|------------------------|-----------------------|
|                         | MINDO/3 CI        | INDO/S CI <sup>a</sup> | Experim. <sup>b</sup> |
| $\tilde{\chi}^2\Pi$     | 0                 | 0                      | 0                     |
| $\chi^2\Sigma^+$        | 1,66              | 2,78                   | 2,82                  |
| $\tilde{\text{B}}^2\Pi$ | 2,53              | 4,31                   | 3,93                  |
| $^2\Pi$                 | 3,08              | 4,75                   | -                     |
| $^4\Sigma^-$            | 4,07              | 6,33                   | -                     |
| $^4\Pi$                 | 4,22              | 3,97                   | -                     |

<sup>a</sup> Reference 17

<sup>b</sup> Reference 3

a  $\dots 1\pi^4 7\sigma^2 2\pi^4$  electronic configuration. The double degenerated  $\tilde{\text{B}}^2\Pi$  state is described by  $\dots 1\pi^3 7\sigma^2 2\pi^4$  electronic configurations. In reactions (1),(2) these both states correlate with the highly excited states of the reagents N + CO (the excitation energies lie in the region of 6,5 - 7 eV).

In order to receive the information about the NCO geometric structure in the excited states, the energy dependences of the ground and excited states on the NCO angle have been calculated. The potential energy curves are

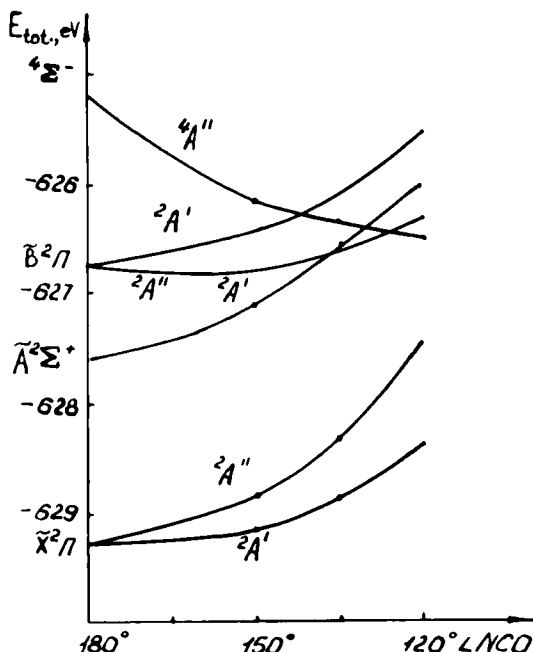


Fig.2. Total energy as a function of bond angle for the ground and some excited states of NCO.

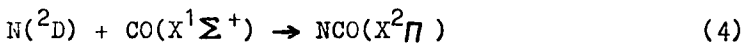
shown in Fig.2, according to which the NCO radical in all lower doublet states has a linear structure. In the quartet  $^4\Sigma^-$  state the NCO radical is bent, because the  $^4\Sigma^-$  ( $^4A''$ ) state energy falls down as the NCO angle decreases to  $110^\circ$ . The shallow minima on the curves for  $\tilde{X}^2\Pi$  state mean a smaller bending frequency as compared with the  $\tilde{A}^2\Sigma^+$  state. As it is seen from Fig.2, the  $\tilde{X}^2\Pi$  state curve slopes up more gently, than the  $\tilde{A}^2\Sigma^+$  curve. This corresponds to the rise of the bending frequencies in transition  $\tilde{X}^2\Pi - \tilde{A}^2\Sigma^+$  ( $539$  and  $681$   $\text{cm}^{-1}$ , respectively)[3].

The reliable MINDO/3 CI energy curves also reproduce the fine structure features of NCO spectrum. The calculated value of  $A^{SO}(\tilde{X}^2\Pi) = -92,794\text{cm}^{-1}$  is in a line with the experimental SOC constant  $-95,59\text{cm}^{-1}$  [3]. Ab initio method gives  $-81,48\text{cm}^{-1}$  [18]. Since the  $\tilde{X}^2\Pi$  state is an almost pure  $G_0$ -configuration (3), this SOC constant is equal to  $A^{SO}(\tilde{X}^2\Pi) = -\alpha_{2\pi}$ , where  $\alpha_{2\pi} = \sum_A c_{2\pi,A}^2 \xi_A$  ( $c_{2\pi,A}$  are the LCAO expansion coefficients of  $2\pi$ -MO of the atom  $A$ ;  $\xi_A$  is a SOC constant for the valence shell electrons of the atom  $A$  [24]). If we took into account only the main contribution of the configuration  $\dots 1\pi^3 7\sigma^2 2\pi^4$ , the SOC constant  $A^{SO}$  for  $\tilde{B}^2\Pi$  state would be equal to  $\alpha_{1\pi} = -106,63\text{cm}^{-1}$ ; that badly agrees with the experimental value ( $-30,8\text{cm}^{-1}$ ). However, the CI calculations show that the  $\tilde{B}^2\Pi$  state contains a considerable admixture of configurations  $\dots 1\pi^4 7\sigma^2 2\pi^2 3\pi^1$ , which have a complicated structure (the  $2\pi^2$  configuration produces  $^3\Sigma^-$ ,  $^1\Delta$  and  $^1\Sigma^+$  structures; if we add one  $3\pi$ -electron, it will lead to the set of the three  $^2\Pi$  states). Taking into account the CI calculation we obtain  $A^{SO}(\tilde{B}^2\Pi) = -35,876\text{cm}^{-1}$ .

The authors [18] have also calculated the SOC splitting of the vibronic levels of the  $\tilde{X}^2\Pi$  state (the Renner-Teller effect). These splittings are very large for unique levels ( $\sim A^{SO}$ ) and considerably smaller for all other levels [18]. The PES for the  $A'$  and  $A''$  components of the  $\tilde{X}^2\Pi$  electronic state of NCO radical are shown in Fig.2. The calculations of Renner-Teller splitting were also carried out by Brown [25]. The results of our calculati-

ons for the variation of the angular momentum proextion on the molecular axcis expectation value  $\langle A''|L_x|A'\rangle$  with the change of the valence angle support the findings of papers [18,25] according to which the value of the parameter  $g_K$  should be close to the value of  $4,1\text{cm}^{-1}$ . The slope of our curve  $L_x$  (4) presented in Fig.3 is slightly higher than the one obtained using Brown's  $g_K$  value [25]. The qualitative agreement between the experimental data [26] and theoretical curves of Brown [25], Peric et al. [18] and our results is rather good (Fig.3). So our MINDO/3 results on the fine structure of  $\tilde{\chi}^2\pi$  state of NCO radical enable a reliable reproduction of a number of experimental findings [3,26], as well as a large-scale MRD-CI calculations [18,25].

Dixon has pointed out [1], that the reactions (1), (2) and (4)



are energetically possible and plausible processes. These suppositions are based alone on the analysis of a symmetry. But a single symmetry analysis cannot give the correct correlation diagrams of reagents and products without the qualitatively reliable understanding of state orbital structures. Our MINDO/3 CI calculation in spite of its apparent drawbacks (the reduced transition energies, the overestimated dissociation energy) gives evidently the qualitatively correct assignment of an orbital character of the initial reagent's and product's states and their correlation along the reaction. It should be noted, that

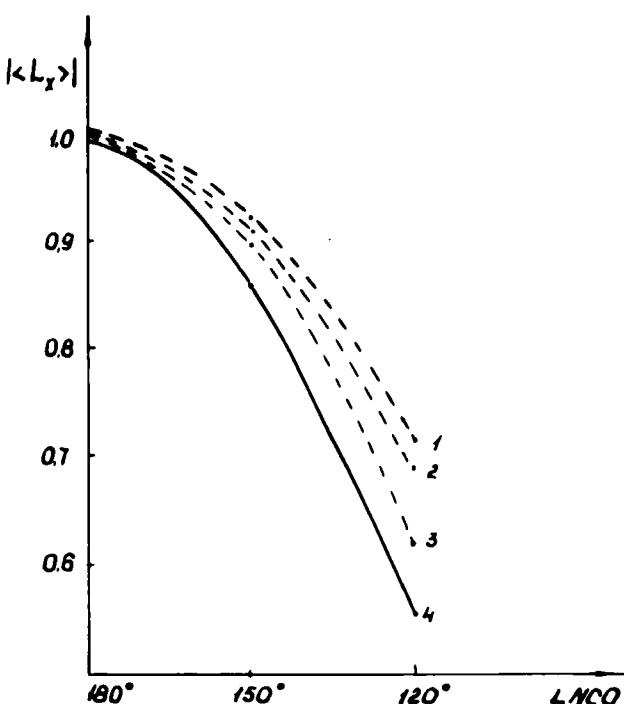


Fig.3. Variation of the expectation value of  $L_x$  with a change of the valence angle. The curves: 1 and 3 - result from ab initio methods [18,25]; 2 - experimental data [26]; 4 - the present work.

the significance and importance of the MO SCF CI semiempirical methods consist rightly of the determination of these qualitative particularities.

The  $N(^2D) + CO(^1\Sigma^+)$  reaction channel. Though the initial state of the reagents  $N(^2D) + CO(^1\Sigma^+)$  gives the term of the  $^2\Pi$ -type, it doesn't correlate with the pro-

und  $\tilde{\chi}^2\Pi$  state of NCO; it is a repulsive term along the reaction. In our calculation it was not taken into account, because its account requires the inclusion of the highly excited configurations. As it is seen from Fig.1, the initial state  $N(^2D) + CO(^1\Sigma^+)$  gives  $^2\Sigma^-$  and  $^2\Delta$  terms, which correlate with the highly excited bonding states of NCO. (The vertical transition energies from the ground state to these ones are  $4,60(^2\Sigma^-)$  and  $4,64\text{eV}$  ( $^2\Delta$ ). These transitions are not observed in the NCO spectrum, because they lie in the UV-region and have very small oscillator strengths. For example, these vertical transition energies calculated by Carsky et al. [17] are equal to 7,61 and 7,92 eV, respectively).

For the linear reaction  $N(^2D) + CO(^1\Sigma^+)$  the adiabatic transition to the NCO ground state is not possible; though the  $^2\Delta$  and  $^2\Sigma^+$  states cross the  $\tilde{\chi}^2\Pi$  state, arising from  $N(^2F)$  term at  $R_{NC} \approx 2,1 \text{\AA}$  (Fig.1), they cannot pass one into another by the adiabatic avoidance. However, such transition is possible at the nonlinear collision. The PES calculation for the N + CO reaction at nonlinear collision (the N-C-O angle is equal to  $150^\circ$ ) is given in Fig.4. As it is seen in Fig.4, the second  $2\Lambda''$  state arising from the entrance channel  $N(^2D) + CO(^1\Sigma^+)$  crosses (point 1) the  $^2\Lambda''$  component of the  $\tilde{\chi}^2\Pi$  state arising from the  $N(^2F) + CO(^1\Sigma^+)$ . The analysis of the CI matrix and the wave functions show that these both  $^2\Lambda''$  states are mixed in this region; the efficient avoided

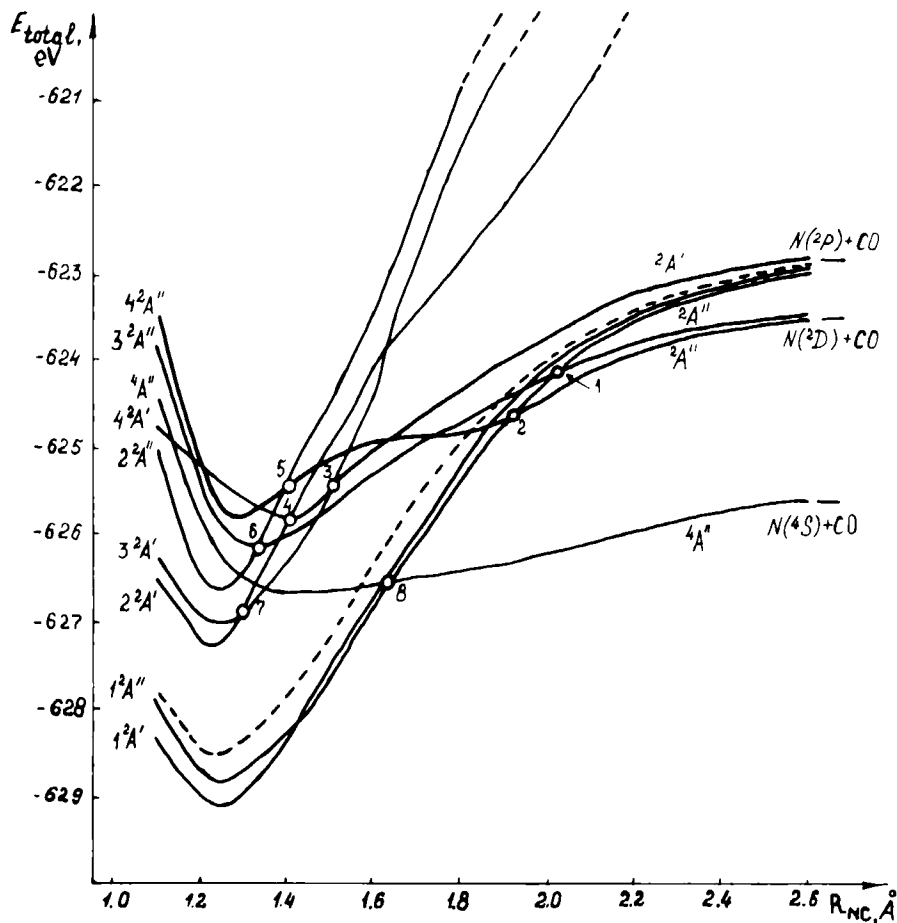


Fig. 4. The low-lying potential energy curves of non-linear NCO ( $\angle \text{NCO} = 150^\circ$ ).

crossing of these states is realized (in Fig. 4 these avoidances are not indicated, in order to simplify the figure and to determine clearer the state orbital structure). The configurational interaction increases beginning from  $\angle \text{NCO} = 170^\circ$  and thus provides a nonadia-

batic reaction process (under the nonadiabaticity we understand the nonlinear perturbation in the entrance channel). That is, the reaction (4) is symmetrically forbidden and becomes nonadiabatically allowed by a nonlinear collision. This circumstance apparently should lead to the excitation of bending vibration in the reaction product  $\text{NCO}(\tilde{\chi}^2\Pi)$ . The low  ${}^2A''$  state arising from the initial reagents  $\text{N}({}^2D) + \text{CO}({}^1\Sigma^+)$  passes through the avoided crossing on  ${}^2A''$  component of the ground  $\tilde{\chi}^2\Pi$  state at  $R_{NC} \approx 1,91 \text{ \AA}$  (point 2 in Fig.4). Thus, at the nonlinear collision the channel  $\text{N}({}^2D) + \text{CO}({}^1\Sigma^+)$  will mainly give the products in the nonexcited  $\tilde{\chi}^2\Pi$  state and only at the expense of nonadiabatic jumps from curve to curve it can lead to the excitation of  ${}^2\Sigma^-$  and  ${}^2\Delta$  states. The reaction yields along that channel depend on collision dynamics, but we shall not discuss them in our paper. One can accept qualitatively, that a part of the colliding particles in the channel  $\text{N}({}^2D) + \text{CO}({}^1\Sigma^+)$  passes through the states  ${}^2\Sigma^-$  and  ${}^2\Delta$  (at least, by the linear collision, if one takes into account the rotational motion).

The  $\text{N}({}^2P) + \text{CO}({}^1\Sigma^+)$  reaction channel. Though the initial reagents  $\text{N}({}^2P) + \text{CO}({}^1\Sigma^+)$  are able to give  ${}^2\Sigma^+$  and  ${}^2\Pi$  states of NCO radical on the symmetry background, their orbital structure doesn't correlate with the states, supposed in the reactions (1) and (2). As it follows from our calculation, the reagents  $\text{N}({}^2P) + \text{CO}({}^1\Sigma^+)$  give the ground  $\tilde{\chi}^2\Pi$  state and the second (in Fig.1) highly excited  ${}^2\Sigma^+$  state.

For the linear collision (Fig.1) the potential curve of  $2^2\Sigma^+$  state crosses the potential curves of the lowest  $\tilde{A}^2\Sigma^+$  and  $\tilde{B}^2\Pi$  states of NCO in the reaction (at  $R_{NC} = 1,5 - 1,55 \text{ \AA}$ ). The  $2^2\Sigma^+$  term doesn't interact with  $\tilde{B}^2\Pi$  state because of their different symmetry. However, as the CI calculation shows, there is only a small mixture of  $\tilde{A}^2\Sigma^+$  and  $2^2\Sigma^+$  states at  $R_{NC} = 1,53 \text{ \AA}$ . Just in the crossing point (point 4') these states have the predominating contributions ( $\sim 98\%$ ) from the configurations  $\dots 76^22\pi^28\sigma$  and  $\dots 76^22\pi^4$ , respectively. The diagonal CI matrix elements for these configurations are distinguished by 0.8eV. An energy coincidence of two  $2^2\Sigma^+$  states at the crossing point  $R_{NC} = 1,53 \text{ \AA}$  is accidental and determined by the small CI contributions from other configurations. Thus, the avoided crossing of two  $2^2\Sigma^+$  states is not effective at linear collision (although formally they must avoid the crossing according to Wigner's theorem). As result of the above mentioned peculiarities this avoided crossing takes place practically in a very narrow region or simply in a single point.

At nonlinear collision (angle 150°) the crossing (point 4) of the two corresponding  $2^2A'$  ( $2^2\Sigma^+$ ) terms are accompanied by a strong CI and a full mixture of configurations  $\dots 76^22\pi^28\sigma$  and  $\dots 76^22\pi^4$ .

As it is mentioned above, the structure of  $\tilde{B}^2\Pi$  state is complicated, that is well confirmed by the calculation of the SOC constant. During the reaction the mixture of the  $2^2\Pi$  states determined by  $1\pi^42\pi^23\pi^1$  configu-

rations leads to an intensive configurational interaction with the  $4^2A'$  state at the change of the NCO angle. At the linear radical structure this  $4^2A'$  state corresponds to the  $2^2\Sigma^+$  term occurring from the dissociation limit  $N(^2P) + CO(^1\Sigma^+)$ . Because of the complicated structure of the  $2^2\Pi$  state a number of the configurations of the same  $A'$  symmetry arised. The mixture of these configurations leads to the efficient avoided crossing of the  $3^2A'$  and  $4^2A'$  states at point 3 just by the small CI matrix elements (at the linear structure it corresponds to the crossing of the  $\tilde{B}^2\Pi$  state component and  $2^2\Sigma^+$  state). Both crossing points 3 and 4 are disposed near the minimum on the potential curve of  $4^2A'(2^2\Sigma^+)$  state, that should lead to the high efficiency of the nonadiabatic transitions. A system passes over and over the crossing points oscillating near the minimum on the potential curve. That must give a quantum yield close to a unity for this process.

Finally, the mixture of  $2^2A'$  and  $3^2A'$  states takes place at the  $R_{NC} = 1,3 \text{ \AA}$  (point 7), that leads to the population of low-lying  $2^2A'$  state (an analog to the  $\tilde{A}^2\Sigma^+$  state in the linear NCO radical).

Since a molecular bending assists the transitions between the terms, the  $\tilde{A}^2\Sigma^+$  state of NCO arising in the reaction will be characterized by the excitation of a bending vibration. It is observed in the NCO chemiluminescence in the region 360-450 nm [15,23].

Besides this, the  $\tilde{B}^2\Pi$  state of NCO radical must be also populated at the nonlinear collision of initial reagents in the  $N(^2P) + CO(^1\Sigma^+)$  channel because of the interaction of its second  $^2A''$  component with the two  $^2A''$  states (the crossing points 5 and 6 in Fig. 4), which diabatically occur from  $N(^2D) + CO(^1\Sigma^+)$  terms. In the nonlinear reaction, as mentioned above, these  $^2A''$  states can arise from the  $N(^2P) + CO(^1\Sigma^+)$  term, taking into account the avoided crossing in points 1 and 2. It is necessary to note, that at the nonlinear collision the low  $^2A'$  state (one of the  $\tilde{X}^2\Pi$  component) arising in the entrance channel  $N(^2P) + CO(^1\Sigma^+)$  will lead straight to the formation of NCO radical in the ground  $\tilde{X}^2\Pi$  state.

Thus, the formation of the NCO radical in low excited states  $\tilde{A}^2\Sigma^+$  and  $\tilde{B}^2\Pi$  (from which the chemiluminescence is observed) takes place in the reaction entrance channel  $N(^2P) + CO(^1\Sigma^+)$ . A population of the  $\tilde{A}^2\Sigma^+$  state results from the adiabatic transitions, whose probability increases at the nonlinear collision of the reagents. The  $B^2\Pi$  state is populated through the nonadiabatic transitions determined by the rovibronic perturbations.

The  $N(^4S) + CO(^1\Sigma^+)$  reaction channel. In this channel the interaction of the reacting particles must be accompanied by a nonadiabatical quartet-doublet ( $^4\Sigma^- - \tilde{X}^2\Pi$ ) transition to the ground state of NCO radical. The calculation of SOC matrix elements [24]

$$\langle ^4\Sigma_{1/2}^- | H_{so} | \tilde{X}^2\Pi_{1/2} \rangle = \frac{1}{\sqrt{3}} \langle ^4\Sigma_{3/2}^- | H_{so} | X^2\Pi_{3/2} \rangle = \frac{1}{\sqrt{12}} B_{2\Pi, 86}$$

shows, that in the crossing point (point 8',  $R_{NC} = 1,7 \text{ \AA}^{\circ}$ ) of  $^4\Sigma^-$  and  $\tilde{X}^2\Pi$  states at the linear reaction, the mixture of these terms caused by SOC is highly efficient. This is connected with a large localization of  $2\pi^-$ - and  $8\sigma^-$ -MO's on 2p-AO of the nitrogen atom and also with a small contribution of the oxygen atom 2p-AO in these MO's:

$$\Psi_{2\pi} = 0.97 \varphi_{2p_y(N)} - 0.21 \varphi_{2p_y(O)},$$

$$\Psi_{86} = -0.82 \varphi_{2p_x(N)} + 0.35 \varphi_{2p_x(O)}.$$

The structure of these MO's determines a large magnitude of the integral  $B_{2\pi, 86} = i \cdot 68,994 \text{ cm}^{-1}$ . The total square of the SOC matrix elements for both sublevels is equal to  $1587,1 \text{ cm}^{-2}$ , that is compared with the SOC matrix element obtained for the nonadiabatic reaction of the nitrogen protoxide decomposition  $N_2O(^1\Sigma^+) \rightarrow N_2 + O(^3P)$  [27].

The appearance of the chemiluminescence is extremely unlikely in this channel, because the SOC matrix elements are very small in the crossing points of  $^4\Sigma^-$  term with  $\tilde{X}^2\Sigma^+$  and  $\tilde{B}^2\Pi$  states. If the transition to the ground  $\tilde{X}^2\Pi$  state doesn't take place at a first passage of the crossing point 8', it will take place at the following passages of this crossing point during vibrations in the vicinity of the minimum on the  $^4\Sigma^-$  state potential curve. The low frequency vibrations with a large amplitude will lead to the repeated passage both through the

point 8' and the crossing points with  $\tilde{A}^2\Sigma^+$  and  $B^2\Pi$  terms. But as the SOC is considerably larger at the point 8', any chemiexcitation will be efficiently quenched in this channel.

The nonadiabatical transition  $\tilde{X}^2\Pi \rightarrow {}^4\Sigma^-$ , induced by SOC, is also possible at the decomposition of NCO molecule. It is obvious, that the CO molecule will be formed in the strongly excited rotational states, because the doublet-quartet transition is accompanied by the sharp change of the valence NCO angle. We suppose, that the dissociation energy  $D_e$  (N-CO) obtained in the experiments [23] corresponds to the formation of the reaction quartet product.

#### R E F E R E N C E S

1. Dixon R.N. - *Phil.Trans.Roy.Soc.* 1960, v.252A, p.165
2. Dixon R.N. - *Can.J.Phys.* 1960, v.38, p.10
3. Herzberg G. *Molecular Spectra and Molecular Structure.* III. *Electronic Spectra and Electronic Structure of Polyatomic Molecules*, Van Nostrand, Toronto, New York, London, 1966.
4. Milligan D.E., Jacox M.E. *J.Chem.Phys.* 1967, v.47, p.5157.
5. Carrington A., Fabris A.R. and Lucas N.J. - *J.Chem.Phys.*, 1968, v.49, p.5545.
6. Carrington A., Fabris A.R., Howard B.J. and al. - *Mol.Phys.*, 1971, v.20, p.961.
7. Saito S. and Amano T. - *J.Mol.Spectrosc.*, 1970, v.34, p.383

8. Charlton T.R., Okamura T. and Thrush B.A. - *Chem. Phys. Lett.*, 1982, v.89, p.98.
9. Copeland R.A., Crosley D.R. and Smith G.P. - "20 Symp. Combust.", Ann Arbor, Mich.", Pittsburgh, 1984, Pa, p.1195
10. Wong K.N., Anderson W.R., Kotlar A.J. and Vanderhoff - *J. Chem. Phys.*, 1984, v.81, p.2970.
11. Dixon R.N., Trenouth M.J. and Western C.M. - *Mol. Phys.*, 1987, v.60, p.779.
12. Louge M.Y. and Hanson R.K. -"20 Symp. Combust., Ann. Arbor, Mich." Pittsburgh, 1984, Pa, p.665.
13. Astbury C.J., Hancock G. and McKendrich K.G. -"9th Int. Symp. Gas Kinet", Bordeaux, 1986, 139/1.
14. Sullivan B.J., Smith G.P. and Crosley D.R. - *Chem. Phys.*
15. Nicholls R.W., Krishnamachari S.L.N. - *Can. J. Chem.*, 1960, v.38, p.1652.
16. Thomson C. and Wishart B.J. - *Theor. Chim. Acta*, 1974, v.35, p.261.
17. Carsky P., Kuhn J. and Zahradnik R. - *J. Mol. Spectrosc.*, 1975, v.55, p.120.
18. Peric M., Hess B.A. and Buerker R.J. - *Mol. Phys.*, 1986, v.58, p.1001.
19. Koch W., Frenking G. - *J. Phys. Chem.*, 1987, v.91, p.49.
20. Dewar M.J.S. and Thiel W. - *J. Amer. Chem. Soc.*, 1975, v.97, p.3978.
21. Ellison F.O. and Matheu F.M. - *Chem. Phys. Lett.*, 1971, v.10, p.332.
22. Zahradnik R. and Carsky P. - *J. Phys. Chem.*, 1970, v.74, p.12.

23. Okabe H. Photochemistry of small molecules.  
John Wiley and Sons. N.Y., Chichester, Toronto, 1978.

24. Muldahmetov Z.M., Minaev B.F. and Kezle G.A. Optical  
and magnetic properties of triplet state. Izd. Nauka,  
Alma-Ata, 1983.

25. Brown J.M. - J.Mol.Spectrosc., 1977, v.68, p.412.

26. Bolman P.S., Brown J.M., Carrington A., Kopp I. and  
Ramsay D.A. - Proc.R.Soc.A, 1975, v.343, p.17.

27. Minaev B.F. - Dep. in KazNIINTI, № 494; 24.08.83,  
Alma-Ata.

Date Received: 04/13/89  
Date Accepted: 05/12/89